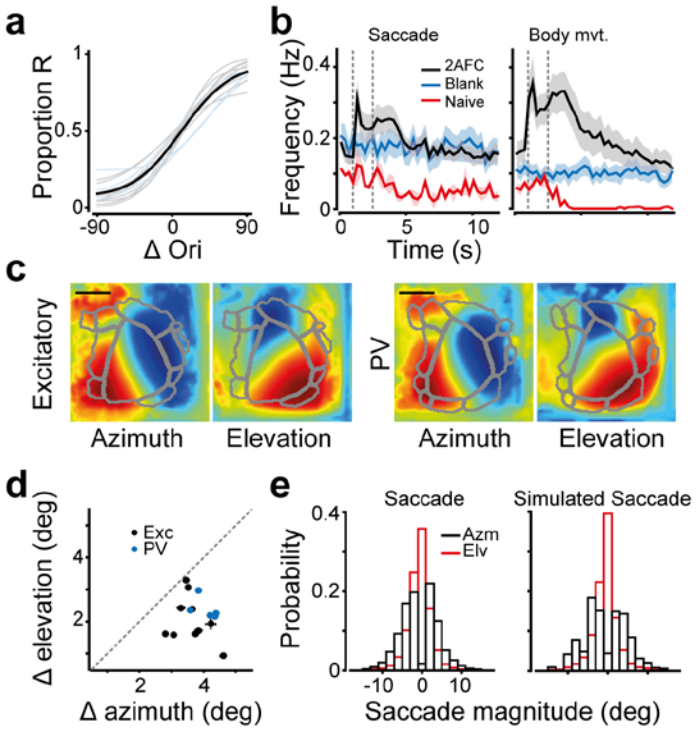

Extended Data Fig. 1. **a**) Psychometric curves. Black line: average across animals (n=12). Individual mice, light color lines: excitatory mice (n=9) light gray, PV mice (n=3) light blue. Sessions with performance >60% and time-out rate <20%. **b**) Distribution of saccades (left) and body movement times (right) in 2AFC (black) and blank (blue) experiments. Red line, naive mice in the same 2AFC tasks (n=2). Vertical dotted lines, open-loop period; shaded bands, s.e. **c**) Average azimuth and elevation maps for excitatory and PV mice. Gray lines, segmentation of visual areas. Scale bar: 1mm. **d**) The amplitude of saccades in azimuth and elevation averaged across all saccades, each dot is the mean for each animal; error bar 95% CI. **e**) Distribution of azimuths and elevations of saccades (left), that were randomly sampled in order to generate simulated saccades (right).

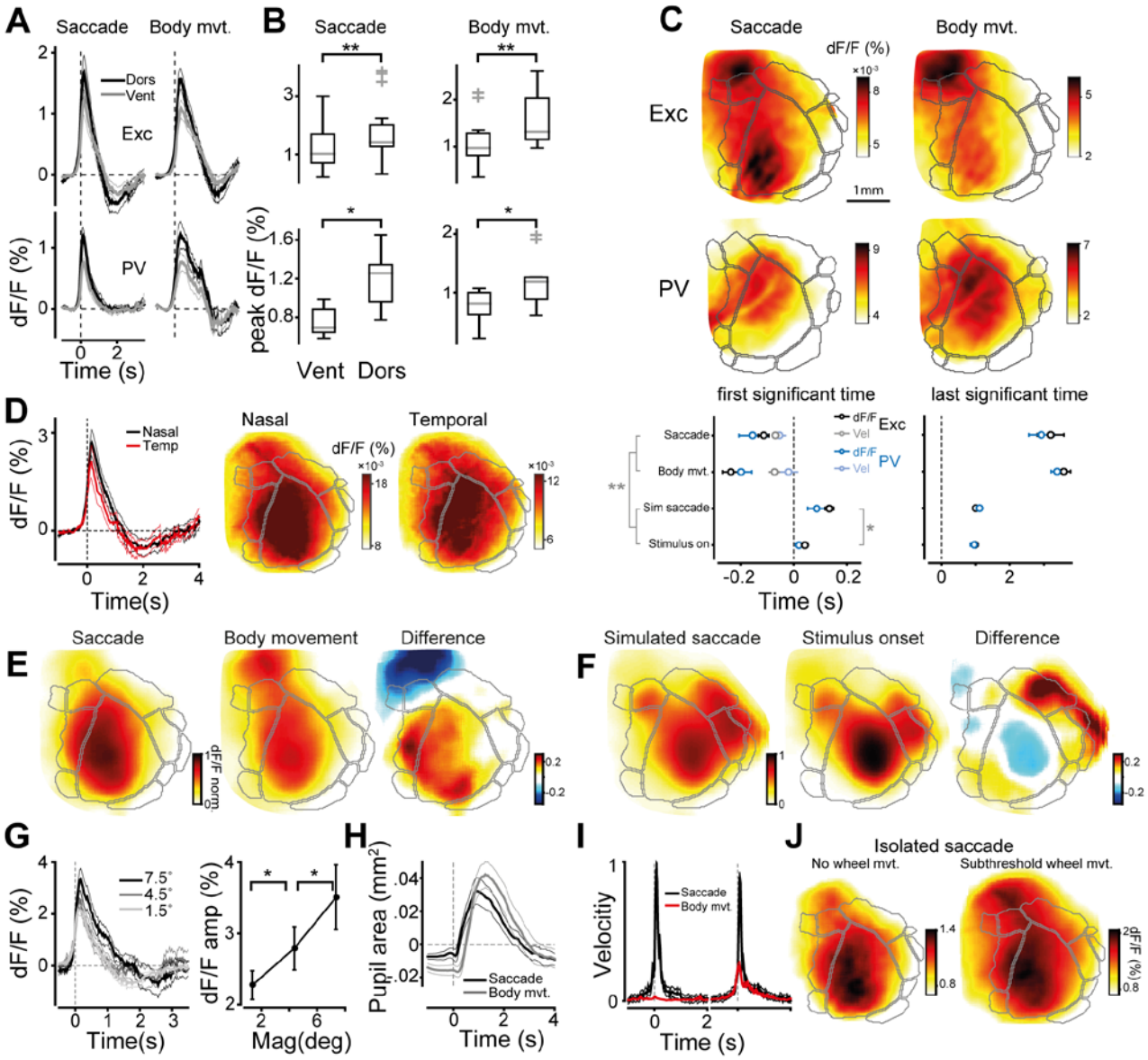

Extended Data Fig. 2. **a**) Isolated saccadic (left) and body movement responses averaged across dorsal (M, PM, AM, RL) and ventral (LM, P, POR) stream areas for excitatory (top) and PV (bottom) mice. **b**) Amplitude difference between ventral and dorsal stream areas at the time of peak response for saccades (left) and body movements (right): p=0.002, p=0.004 (saccades and body movement, for excitatory mice t-test, n=10); p=0.03, p=0.02 (PV, n=5). Box and whisker plots, central line for the median, top-bottom for 25-75 percentiles, error bars extend to the most extreme data points, excluding outliers (gray crosses). **c**) Top: pre-event activity pattern for saccades (left, t= [-100, 0]ms) and body movements (right, t= [-100, 0]ms) for excitatory (top) and PV (middle) mice. Bottom: first (left) and last (right) time point significantly different from the activity in the [-0.8 -0.3]s window before saccade and body movement and in the [-0.3 0]s window for stimulus onset and simulated saccades. For Exc: saccades, -110±20ms; body movements -237±31ms; n=10. For PV: saccades, -153±52ms; body movements -200±40ms; n=5. Delay of simulated saccade response relative to its onset: 133±14ms. Gray dots, detection time of saccades and body movements from movement velocities (Methods). **d**) Left: activation maps for nasal and temporal

saccades in the saccade ROI (Extended Data Fig. 10j-n); t-test for difference in the peak response amplitude: p=0.22 (n=10). Right: response maps for nasal and temporal saccades at the time of peak response. **e**) Average response patterns (n=15 mice) at the time of peak amplitude for saccades and body movements and their difference normalized to [0, 1], and derived as in Extended Data Fig. 10j-n (Methods). **f**) Same as (e) for simulated saccades and for stimulus onset. **g**) Left: Saccadic responses to three different saccade amplitudes (1.5°, 4.5°, and 7.5°; shades of gray) in saccade ROI. Right: amplitude of saccadic responses at the time of peak response for different saccade magnitudes (t-test p=0.01, n=10); error bands, s.e. **h**) Changes of pupil area for saccades and body movements. Amplitudes are normalized (subtracted) relative to the session average (Methods). **i**) Velocities below the detection threshold can modulate the amplitude of the isolated saccadic response, as shown for trials with small (left) or large (right) subthreshold wheel velocity (Methods); error bands, s.e. **j**) Saccadic response maps for corresponding panels in (i).

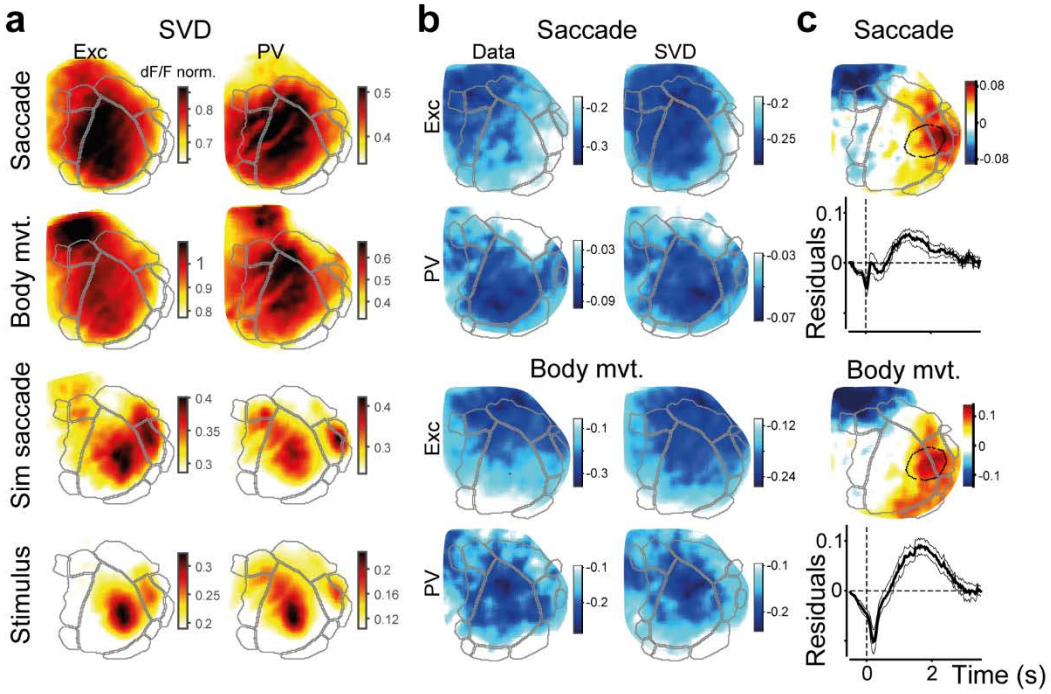

Extended Data Fig. 3. Singular Value Decomposition (SVD). **a**) SVD model (Methods) for different events (rows) for excitatory (left, n=10) and PV (right, n=5) mice. Explained variance (EV, Methods) of SVD for saccades: 87.8±1.3% (Exc, s.e.), 76±2% (PV); for body movements: 88.5±3.9%, 78±3%. **b**) Response maps for saccades (top) and body movement (bottom) isolated from other events (Methods), at the time of max delayed suppression. Left, data; right, SVD. **c**) Map of SVD residuals estimated using the time point of peak residual amplitude in the stimulus motion ROI (dotted contours) (t=1.4s and t=1.7s for saccade and body movement). Time-series of the residuals in the stimulus motion ROI are shown below the maps. Maximum normalized residual amplitude for saccades: 0.05±0.01 (s.e., t-test $p<0.01$; n=10) and for body movements: 0.09±0.01 (s.e., t-test $p<0.001$). All dF/F values reported here are normalized (Methods).

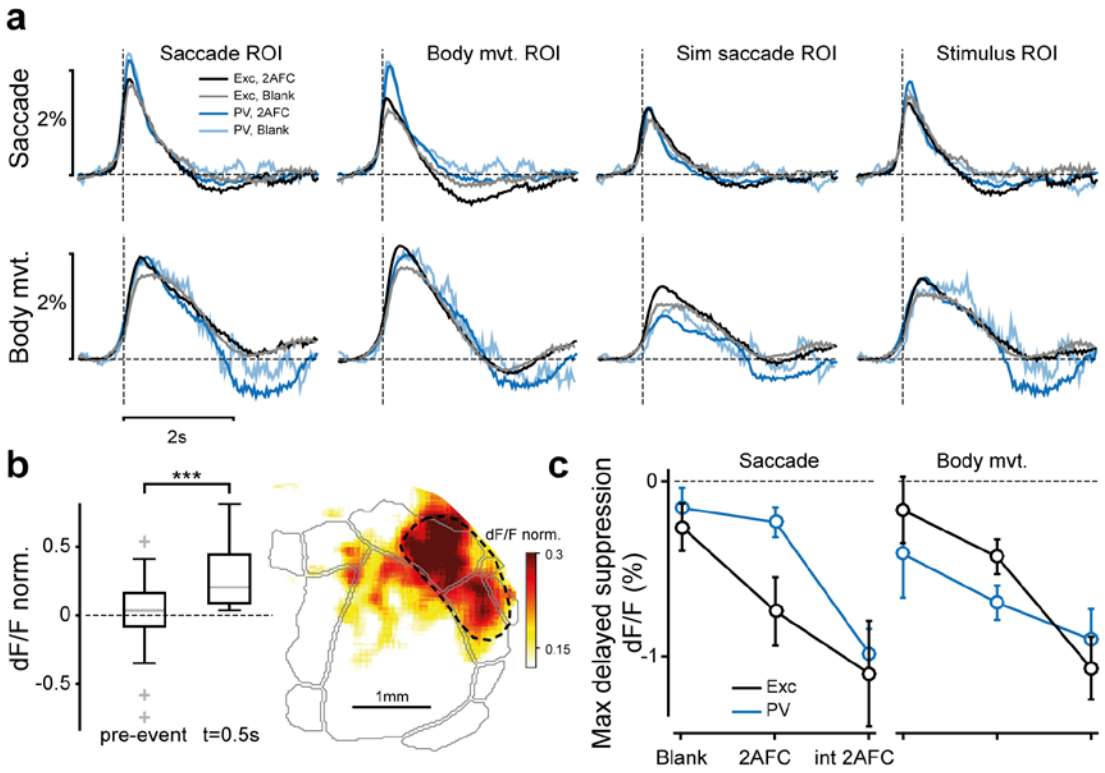

Extended Data Fig. 4. Isolated responses in 'blank trials' vs 2AFC conditions. **a**) Responses to saccades (top) and body movements (bottom) in 4 different ROIs (columns), averaged across mice that have been tested in both conditions (n=5, Exc; n=4, PV). Black and gray for excitatory mice, dark and light blue for PV mice, during 2AFC and blank experiments, respectively (peak response in blank versus 2AFC, t-test, p>0.5). FWHM was also unchanged in 2AFC vs blank conditions (t-test, p>0.5). **b**) Left: difference of 2AFC-blank saccadic response amplitudes, before the saccade ([-270:-130]ms) and after, at t=0.5 (n=6, $p<10^{-3}$) with a spatial localization in motion sensitive areas[27] (right panel, dashed contour line). **c**) Comparing the mean amplitude of max delayed suppression in isolated events during blank trials, in isolated events during 2AFC trials, and in interacting saccade-body movement events in 2AFC trials, in saccade and body movement ROIs, for excitatory (black) and PV (blue) mice. Error bars, s.e. Delayed suppression was significantly reduced in blank condition, -0.34±0.11%, not different from the pre-event baseline activity (t-test, p=0.1, n=5). The max amplitude of the delayed suppression was lower than baseline for saccades (-0.7±0.2%, Exc, t-test p=0.004; -0.23±0.08%, PV, t-test p= 0.051) and for body movement (-0.4±0.1%, Exc, t-test p=0.001; -0.7±0.01%, PV, n=4, t-test p= 0.005). Time of maximum delayed suppression for saccade (1.9±0.13s, Exc; 2.4±0.22s, PV), and for body movement (2.2±0.08s, Exc; 2.6±0.09s, PV, n=4).

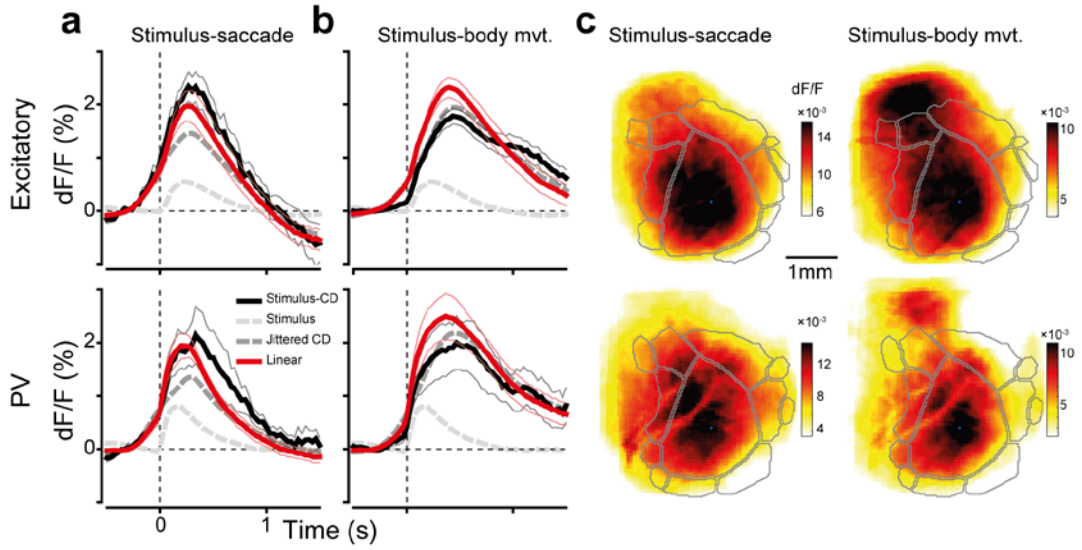

Extended Data Fig. 5. Linear prediction of stimulus-CD interactions: **a**) Stimulus-saccade interaction in stimulus ROI, linear model (red, Methods) and data (black) for excitatory (top) and PV (bottom) mice. Peak response amplitude, average across mice: 2.1±0.22 (dF/F (%) ±s.e., Exc); 1.9±0.5, PV. Comparable response activations were observed for PV interneurons: peak response amplitudes were 2.4 and 2.4 times larger than the contrast response; t-test, p=0.06 and 0.05 respectively for saccade and body movement; n=5; FWHM: 0.53±0.03 and 0.71±0.03s; t-test w/wo contrast response: p=0.3 and p=0.2. **b**) Same as (a) for stimulus-body movement interactions in stimulus ROI. Peak response amplitude, average across mice: 1.7±0.14 for excitatory; 1.9±0.46 for PV. **c**) Activation maps for corresponding panels in (a) and (b) at the time of peak response.

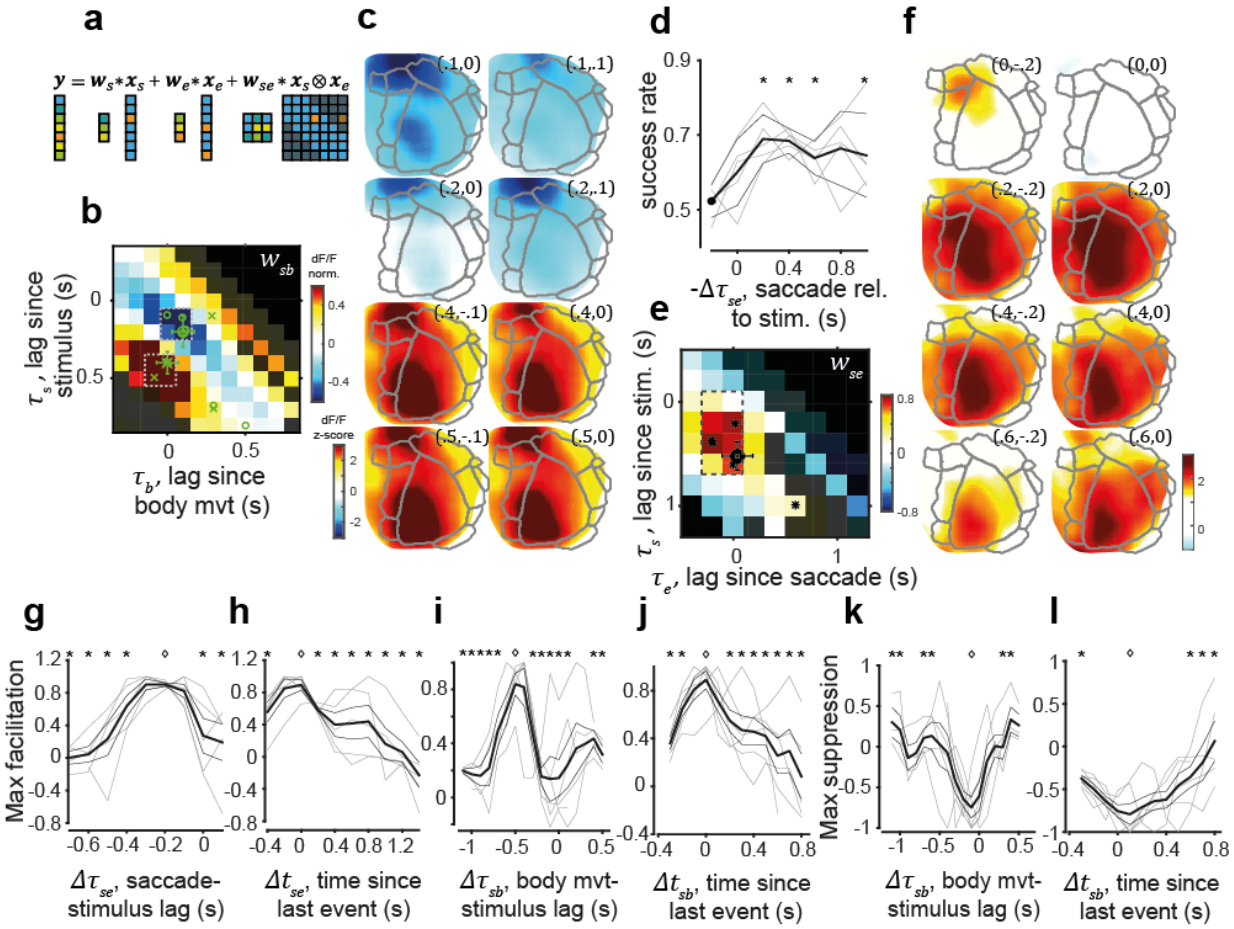

Extended Data Fig. 6. GLM predictions for stimulus-CD interactions. **a**) GLM with example stimulus-CD (eye movement) nonlinear interaction term (Methods). Inputs x_s, x_e are convolved ($*$) with respective kernels w_s, w_e, and outer product $x_s \otimes x_e$ is convolved with w_{se} along the diagonal. **b**) Normalized stimulus-body movement interaction kernel w_{sb} estimated from isolated stimulus-body movement pairs, average of excitatory mice (n=6). Nonlinear interaction of stimulus and body movement occurring with a fixed relative lag, $\Delta\tau_{sb} = \tau_b - \tau_s$, corresponds to values along a diagonal parallel to main, with Δτ>0 (elements above diagonal) when body movement happens first. Elements in black are unattainable since the earliest body movement could happen 0.5s before the stimulus, dim-color elements are estimated from n<5 animals. Green circles, maximum suppression lags of individual animals; large circle, their median (τ_b=0.1±0.07s, τ_s=0.2±0.1s, median-based s.e.). Green crosses, maximum facilitation lags of individual animals; large cross, their median (τ_b=0±0.07s, τ_s=0.4±0.07s). Elements within two dashed white squares are used for predictions in (c) **c**) Amplitude of the nonlinear component during body movement-stimulus interaction predicted by the GLM, each frame of a given animal is normalized by standard deviation of its dF/F pixel values and averaged across animals; frames correspond to kernel elements marked with a dashed line in (b), lags (τ_s,τ_b) (s) are shown in the upper-right corner. **d**) Success rate on trials with an isolated stimulus-saccade interaction as a function of saccade time-time relative to stimulus onset. Black lines - population average and confidence intervals, faint lines - individual animals. Success rates significantly better than that at $\Delta\tau_{se}$=-0.2s are marked with asterisks (U-test, α=0.05). **e**) Normalized stimulus-eye movement interaction kernel w_{se} estimated from isolated pairs, average of excitatory mice (n=5). Maximally facilitating elements of individual animals are shown with black asterisks:

population mean, black circle (τ_e=0.04±0.15s; τ_s=0.52±0.14s; s.e.). Elements within dashed black rectangle are used for prediction in (f). **f**) Amplitude of the nonlinear component during saccade-stimulus interaction predicted by the GLM, normalization as in (c), frames correspond to the highlighted kernel elements in (e), lags (τ_s, τ_e) (s) are shown in the upper-right corner. **g**) Maximum facilitation as function of relative lag between saccade and stimulus $\Delta\tau_{se} = \tau_e - \tau_s$. Black lines - population average with confidence intervals, faint lines - individual animals, asterisks show values significantly different from population maximum (diamond) (U-test, α=0.05). **h**) Maximum facilitation as function of time since the saccade or stimulus onset, whichever happened last, Δt_{se}= min(τ_e, τ_b), same colors and statistical tests as in (g). **i,j**) Analogous to (g,h) but for maximum facilitation in the body movement-stimulus interaction. **k,l**) Analogous to (g,h) but for maximum suppression in the body movement-stimulus interaction.

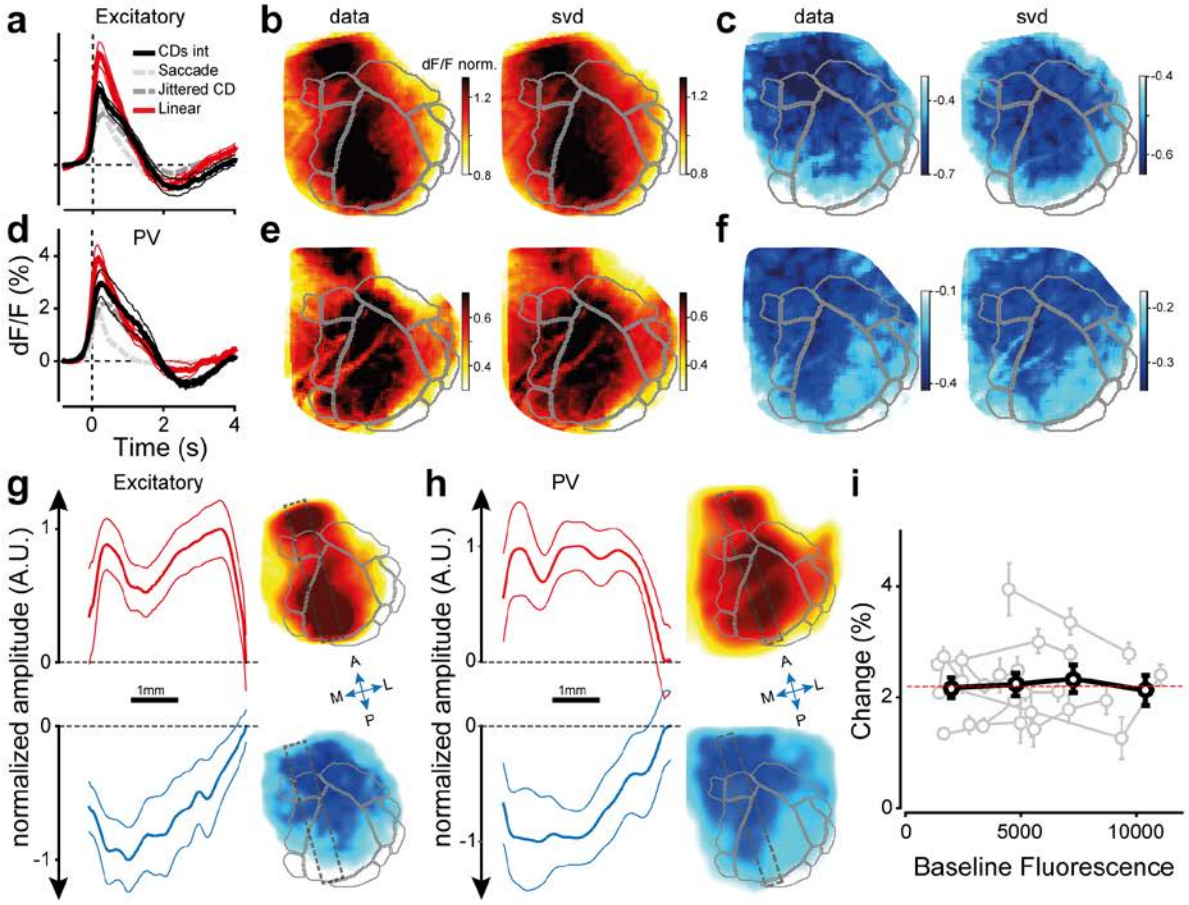

Extended Data Fig. 7. Linear prediction of CDs interactions. **a**) Linear model (red, Methods) and data (black) for excitatory mice. **b**) Activity maps at the time of peak response for interacting CDs in excitatory mice. Left panel, data; right panel, SVD (Methods). **c**) Activity maps at the time of max delayed suppression. **d-f**) Same as a-c for PV mice. **g-h**) Left panels: comparison of spatial activations at times of peak response (top-left) and max suppression (bottom-left) in excitatory (g) and PV (h) mice. Maps in the right panels have been smoothed relative to (b,c,e,f) to reduce pixel noise. Left-panels, responses are pixel averages within the dashed black rectangles shown in right-panel maps. Error bands are s.e. Values are normalized between zero and ±1. **i**) GCaMP responses do not saturate during CD interactions (Methods). Peak fluorescence change (%) during interacting CDs as a function of the associated baseline fluorescence (averaged across trials) for individual mice (gray lines and symbols; error bars, 95% CI) and for the average across animals (black line and symbols; error bars, s.e.; n=9). Red dashed line, linear fit to data from all mice.

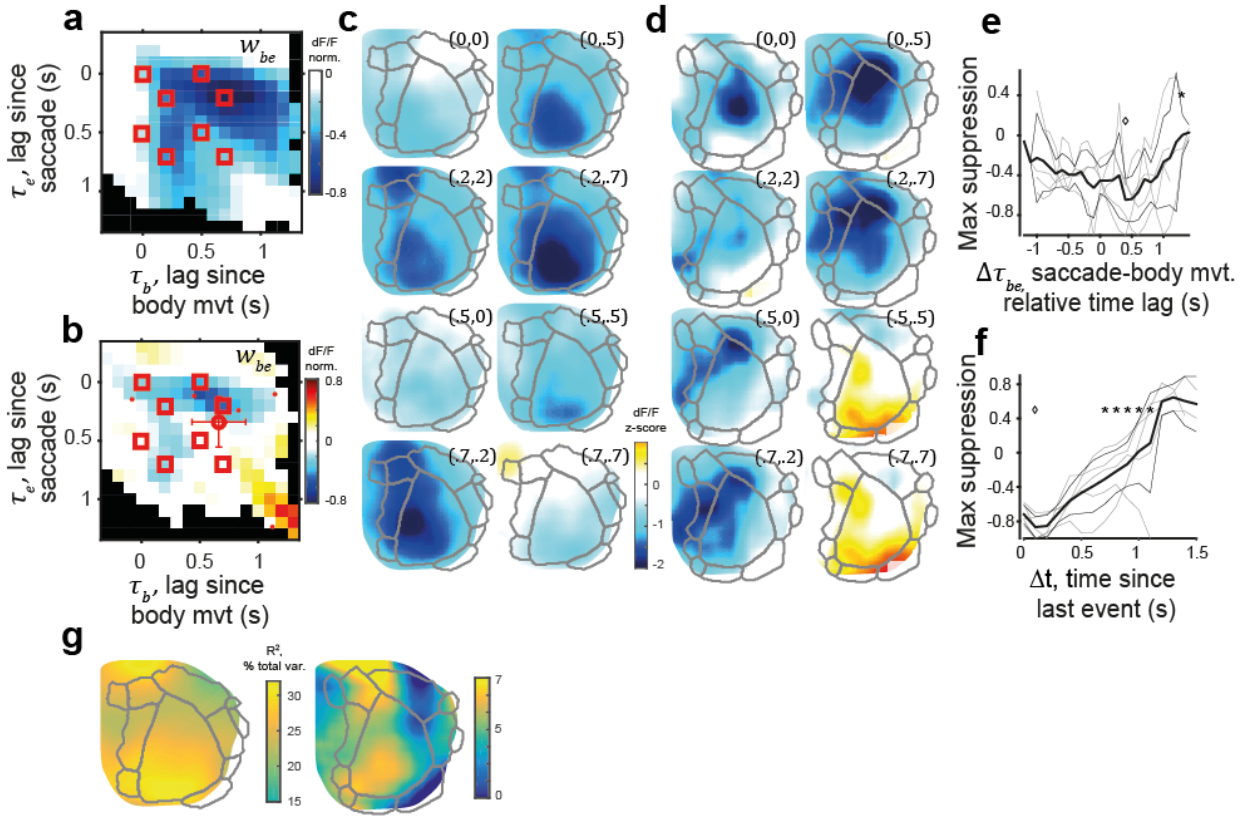

Extended Data Fig. 8. GLM predictions for CD-CD interactions. **a**) Normalized saccade-body movement interaction kernel averaged across excitatory mice (n=8) (Fig. 2e) with elements corresponding to (c) in red boxes. **b**) Population average of normalized saccade-body movement interaction kernel, PV mice (n=5) with elements corresponding to (d) in red boxes. Red dots, maximum suppression lags of individual animals; circle with error bars, average lags across animals (τ_b=0.66±0.23s, τ_e=0.34±0.22s, s.e.). Masked values (black) for n<5 animals. **c**) Amplitude of nonlinear saccade-body movement component, eight example frames, red square in (a); insets for lags (τ_s,τ_b); average across excitatory mice. Frames of individual mice are normalized to the standard deviation of dF/F in that frame. **d**) Same as (c), but for PV mice; same color bar. **e**) Maximum suppression as a function of $\Delta\tau_{be} = \tau_b - \tau_e$, for PV mice, similar to Fig. 2f. Black lines, population average with confidence intervals. Faint lines, individual animals. Asterisks, lags with suppression significantly different from curve minimum (diamond), (U-test, α=0.05). Average $\Delta\tau_{be}$ of minimum: 0.34 ± 0.22 s.e. **f**) Maximum suppression as function of time since the last event, $\Delta t = min(\tau_b, \tau_e)$. Colors as in (e); asterisks, Δt with data for n=5 animals significantly different from average curve minimum (U-test, α=0.05). Average time: Δt=0.28±0.21, s.e. **g)** Left. Average variance explained (R^2) by the full model with interactions, excitatory mice (n=8). Right. Same for PV mice (n=5), where kernels are more strongly penalized by regularization (Methods).

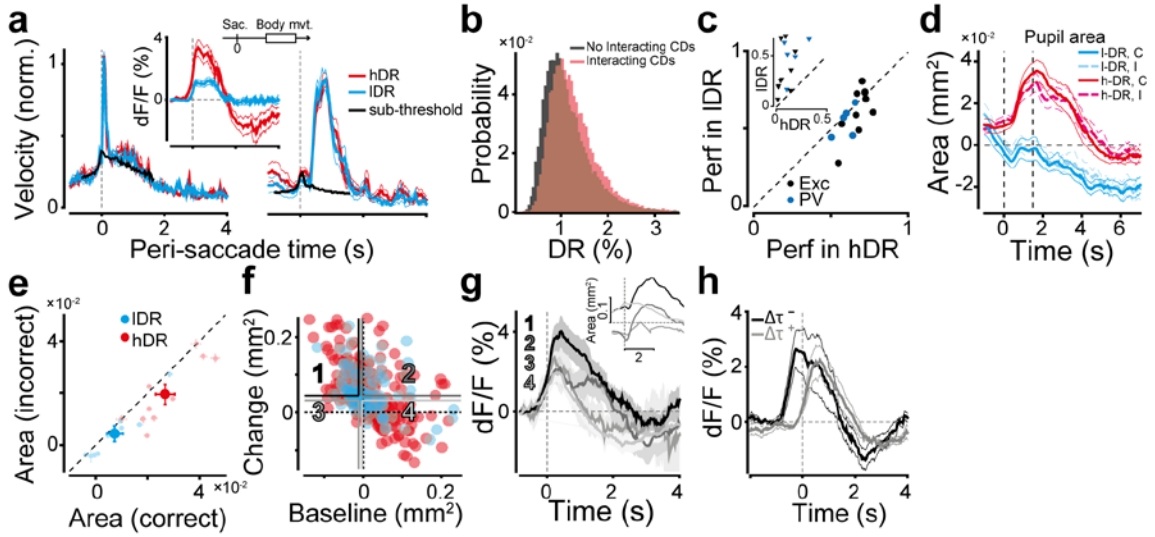

126 Extended Data Fig. 9. **a**) The occurrence of CDs was neither sufficient nor necessary for high DR values.
127 Velocity of interacting saccade (left) and body movements (right) aligned to the time of saccade, for $\Delta\tau^+$
128 lag, separated for high and low DR. Middle-top inset, schematic of the temporal window for body
129 movements relative to zero-time saccades. Equal saccadic and body movement velocities dF/F are
130 associated to different responses in high and low DR states (middle inset, red-blue for high-low DR). Black
131 curve: subthreshold velocity of saccades around isolated body movements (left), and subthreshold
132 velocity of wheel movements around isolated saccades (right), replotted from insets in Fig. 1f. The
133 subthreshold movement components are not a unique feature of isolated events (Fig. 1f, Extended Data
134 Fig. 2i) and are similarly present during interactions. **b**) Probability distribution of DR in trials with or
135 without interacting CDs (t-test $p<10^{-4}$). **c**) Performance in high versus low DR across all trials, excluding
136 timeouts. Inset: proportion of timeout trials in high versus low DR. **d**) Pupil area for high and low DR, with
137 trials separated by choices: correct, solid line; incorrect, dashed line **e**) Maximum amplitude of pupil area
138 in correct versus incorrect trials separated to high and low DR (pale symbols: individual mice; solid
139 symbols: average across mice; error: s.e., n=10). **f-g**) Same as Fig. 3f,g, for PV mice. **h**) Same as Fig. 4h, for
140 PV mice.

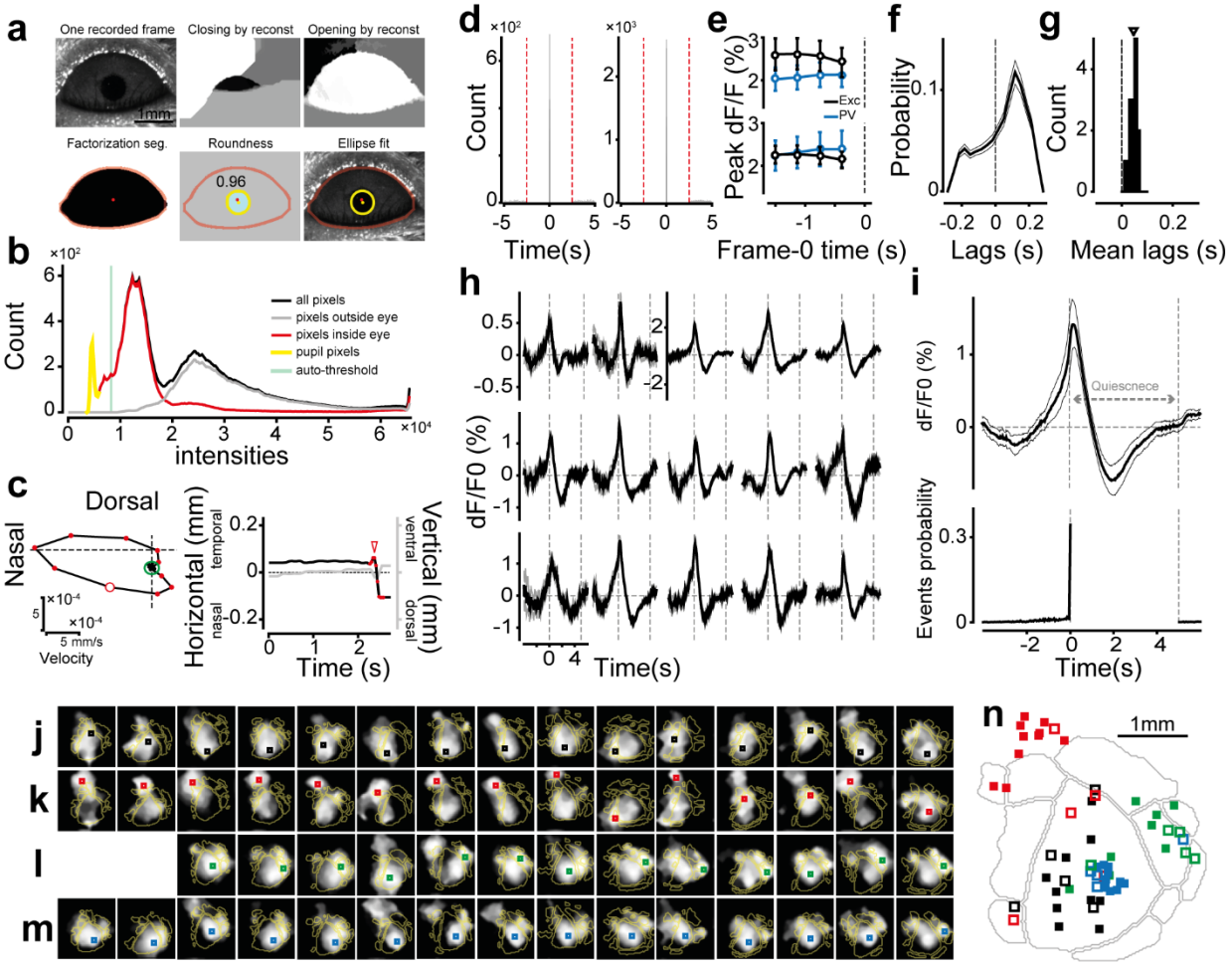

Extended Data Fig. 10. **a**) Frame-by-frame processing steps to estimate the area and center position of the pupil. **b**) Threshold estimation based on intensity distributions within and outside the eye segment (Otsu 1979). **c**) Saccade detection by adaptive elliptic thresholding (left, Methods): black line, velocity trace during a trial; large red dot, time of saccade detected outside the elliptic threshold (green circle). Small red dots, potential saccades also outside the elliptic threshold, but excluded based on a minimum-amplitude threshold (Methods). Right: Pupil position over time (black and gray for azimuth and elevation, respectively). Arrowhead indicates the time of the detected saccade (the large red dot on the left panel); small red dots, time-points as in left panel. Horizontal dotted line, average pupil position across trials. **d**) Histogram count of time-aligned isolated saccades (left) and body movements (right) and of events outside the isolation window (red dashed lines), not visible in this y-scale. **e**) Peak responses of isolated saccades (top) and body movements (bottom) do not depend on the temporal distance from the detected event of the temporal window used for frame-0 correction (Methods). Error bars, s.e. **f**) Probability of saccade-body movement lags to be within a [-0.25, 0.25]s window from each other; average across animals (n=15). Negative times: saccades before body movements. **g**) Distribution of the mean lag across animals; triangle, grand mean, 45ms, t-test, $p<10^{-4}$. **h**) Estimating an appropriate duration for the isolation window (ERA analysis) using a "quiescence period": trial averaged responses for individual mice aligned to the beginning of a 5s period (t=0, and vertical dashed lines) with no detected saccade or body movement (quiescent period). Error bars, 95% CI. **i**) Top: average of responses shown in (h), the response

goes back to baseline at the end of the quiescent period. Bottom: probability of events happening outside the quiescence period, average across animals. The spike at zero is expected given how the quiescent period has been defined. **j-m**) Average of thresholded amplitude maps (Methods) used to define ROIs for ERAs shown in Fig. 1f. **j**) Saccade, **k**) body movement, **l**) simulated saccade, **m**) stimulus onset. Colored square, location of the peak responses. **n**) All ROIs for all mice after retinotopically aligning the maps. Filled symbols, excitatory mice; empty symbols, PV. Black, red, green and blue, same as (j-m).